

See discussions, stats, and author profiles for this publication at: <https://www.researchgate.net/publication/228810212>

Investigation of the Excited-State Dynamics of Radical Ions in the Condensed Phase Using the Picosecond Transient Grating Technique

ARTICLE *in* THE JOURNAL OF PHYSICAL CHEMISTRY A · JULY 1997

Impact Factor: 2.69 · DOI: 10.1021/jp972066v

CITATIONS

30

READS

5

2 AUTHORS, INCLUDING:



Eric Vauthey

University of Geneva

223 PUBLICATIONS 4,347 CITATIONS

SEE PROFILE

ARTICLES

Investigation of the Excited-State Dynamics of Radical Ions in the Condensed Phase Using the Picosecond Transient Grating Technique

Jean-Claude Gummy and Eric Vauthey*

Institute of Physical Chemistry of the University of Fribourg, Pérolles, CH-1700 Fribourg, Switzerland

Received: June 25, 1997; In Final Form: August 26, 1997[®]

A study of the dynamics of ground-state recovery of the perylene radical cation ($\text{Pe}^{\bullet+}$), of perylene radical anion ($\text{Pe}^{\bullet-}$), and of anthraquinone radical anion ($\text{AQ}^{\bullet-}$) is reported. In boric acid glass, the excited-state lifetime of $\text{Pe}^{\bullet+}$ is 35 ± 3 ps, while in concentrated sulfuric acid, it is smaller than 15 ps, the time resolution of the experimental setup. The excited-state lifetime of $\text{Pe}^{\bullet+}$, $\text{Pe}^{\bullet-}$, and $\text{AQ}^{\bullet-}$ generated by photoinduced intermolecular electron-transfer reaction in MeCN is shorter than 15 ps. In the case of $\text{Pe}^{\bullet-}$, the uncomplete ground-state recovery is ascribed to the occurrence of electron photoejection. The free ion yield in the intermolecular electron-transfer reaction between 9,10-dicyanoanthracene (DCA) and two electron acceptors was measured in a two-pulse experiment, where the second pulse excited the ensuing $\text{DCA}^{\bullet-}$. This excitation has no influence on the magnitude of the free ion yield, indicating a short excited-state lifetime of $\text{DCA}^{\bullet-}$ relative to the time scale of back electron transfer and ionic dissociation. A red emission, ascribed to the fluorescence of protonated Pe, was detected in boric acid glass and sulfuric acid. No fluorescence that could be clearly ascribed to $\text{Pe}^{\bullet+}$ could be observed.

Introduction

Open-shell organic radical ions play a crucial role in a large variety of chemical processes. Although the photochemistry of these species has been intensively studied, especially in solid matrixes at low temperature,¹ little is known about the dynamics of their excited states. The absence of the inverted region for highly exergonic bimolecular electron transfer (ET) quenching reactions in solution has sometimes been explained by the production of electronically excited ions.^{1–3} However, the formation of such excited ions could not be confirmed experimentally with either absorption or fluorescence techniques.^{2,3} Fluorescence from radical cations has been observed in the gas phase^{4,5} and in matrixes at low temperature.⁶ In the condensed phase at room temperature, there have been only very few

reports of fluorescence from radical ions.^{7–9} Recently, Breslin and Fox¹⁰ have shown that, among those reported emissions in solution, several were not genuine. For example, the fluorescence ascribed to anthraquinone radical anion ($\text{AQ}^{\bullet-}$) was actually due to bianthrone dianion and that assigned to 9,10-dicyanoanthracene anion ($\text{DCA}^{\bullet-}$) originated from 10-cyanoanthrolate. Moreover, no transient with nanosecond lifetime could be observed upon excitation of $\text{AQ}^{\bullet-}$ at wavelengths above 500 nm. The absence of luminescence and of transient with nanosecond lifetime is generally explained by a fast nonradiative transition to the ground state favored by the small energy gap between the D_1 – D_0 states.

Very recently, Majima and co-workers¹¹ reported excited-state lifetimes of $\text{AQ}^{\bullet-}$, $\text{DCA}^{\bullet-}$, and phenazine radical ions of the order of 4 ns. These lifetimes were not measured directly but were estimated from the rate constant of ET quenching of the excited ions by an electron acceptor using a combination

* Corresponding author. E-mail: Eric.Vauthey@unifr.ch.

[®] Abstract published in *Advance ACS Abstracts*, October 15, 1997.

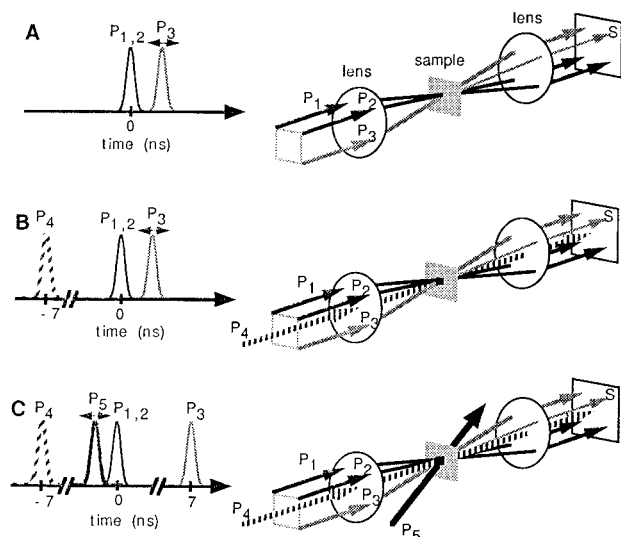


Figure 1. Pulse sequences and geometries (A) for the transient grating experiments with $\text{Pe}^{+\bullet}$ in boric acid glass and H_2SO_4 , (B) for the transient grating experiments with ions generated by photoinduced ET, and (C) for probing the density grating formed at different time delays after a bleaching pulse ($P_{1,2}$, transient grating pump pulses; P_3 , probe pulse; P_4 , UV pulse; P_5 , bleaching pulse; S, signal pulse).

of pulse radiolysis and nanosecond flash photolysis. In this case as well, no transient was observed upon excitation of the radical ions.

In this paper, we report on the investigation of the dynamics of ground-state recovery of the radical cation of perylene ($\text{Pe}^{+\bullet}$) in a boric acid glass, in sulfuric acid, and in acetonitrile (MeCN), of perylene radical anion ($\text{Pe}^{-\bullet}$), and of $\text{AQ}^{-\bullet}$ in MeCN, using the picosecond transient grating technique. This method was preferred to the more conventional transient absorption spectroscopy because of its superior sensitivity. A simple experiment allowing an indirect estimate of the excited-state lifetime of radical ions is also described.

Experimental Section

Transient Grating. The transient grating setup has been described in detail elsewhere.^{12,13} Briefly, the second harmonic output at 532 nm of a passive/active mode-locked and Q-switched Nd:YAG laser (Continuum PY-61-10) was split into three parts. Two parts of equal intensity (P_1 and P_2) were time coincident and were crossed on the sample with an angle of 2° to generate the grating. The third part (P_3) was sent along a time delay line before striking the grating in a folded BOXCARS geometry (see Figure 1a). For probing at 545 nm, this time-delayed pulse was Raman-shifted in CCl_4 . The energy of the pump pulses was about 20 μJ , and that of the probe pulse was at least 10 times smaller. The beam radii on the sample were around 1 mm, and the pulse duration was about 25 ps. The polarization of each pulse could be controlled with a combination of Glan-Taylor polarizers and half-waveplates.

For experiments in MeCN, the ET reaction was initiated with a 25 ps pulse at 355 nm with an energy between 0.5 and 1 mJ. This UV pulse (P_4) arrived on the sample 7 ns before the two 532 nm transient grating pulses. Its radius on the sample was around 2 mm.

Free Ion Yields. The free ion yields were determined using photoconductivity. The photocurrent cell has been described in detail elsewhere.¹⁴ Excitation was carried out with a Q-switched Nd:YAG laser (JK Laser Model 2000) generating 10 mJ pulses at 355 nm with 20 ns duration.

Fluorescence. Fluorescence spectra were measured using a CCD camera (Oriel Instaspec IV) connected to a $1/4$ m imaging

spectrograph (Oriel Multispec). All the emission spectra were corrected for the spectral sensitivity of the CCD camera.

Samples. Perylene (Pe) and anthraquinone (AQ) were recrystallized from benzene. Tetracyanoethylene (TCNE) was recrystallized from chlorobenzene and sublimed. Fluorene (FLU) was recrystallized from ethanol. Anisol (ANI) and *N,N*-dimethylaniline (DMA) were vacuum-distilled. 9,10-Dicyanoanthracene (DCA, Aldrich) and 1,4-diazabicyclo[2.2.2]octane (DABCO) were sublimed. Crystal violet (CV), boric acid (puriss.), sulfuric acid (95–97%, Merck, pro analysi), acetonitrile (MeCN, UV grade), and methanol (MeOH, UV grade) were used without further purification. Unless specified, all products were from Fluka.

The Pe-doped boric acid glass was prepared by melting at 210–220 $^\circ\text{C}$ a mixture of boric acid and Pe between two quartz plates. The resulting metaboric acid glass was 0.1 mm thick and was of good optical quality. The Pe concentration was measured spectroscopically to be around 5×10^{-4} M. The $\text{Pe}^{+\bullet}$ was prepared by irradiating the doped glass with nanosecond laser pulses at 355 nm.¹⁵ The absorption spectrum of the ensuing pink glass exhibited the bands of Pe as well as those of $\text{Pe}^{+\bullet}$, i.e., a strong band at 543 nm and weaker bands between 580 and 765 nm.¹⁶ The absorbance of the sample at 532 nm was 0.09.

In sulfuric acid, $\text{Pe}^{+\bullet}$ was readily prepared by adding Pe to the acid. Solutions with various $\text{Pe}^{+\bullet}$ concentration were used, and the optical path length was adjusted to achieve an absorbance at 532 nm between 0.1 and 0.2.

In MeCN, the concentration of the parent neutral compound was adjusted to obtain an absorbance at 355 nm between 0.1 and 0.2 on 1 mm, the cell thickness. With Pe and AQ, the quencher concentration was 0.2 and 0.1 M, respectively.

Data Analysis. The transient grating technique is a four-wave mixing method, and therefore the signal intensity depends on the third-order nonlinear optical susceptibility tensor $\chi^{(3)}$ of the sample.¹⁷ The intensity of the diffracted signal, $I_d(t)$, can be expressed as^{18,19}

$$I_d(t) = \int_{-\infty}^{+\infty} I_{P_3}(t - t'') \times \sum_m \{ C_m \chi_{ijkl}^{(3)}(m) \int_{-\infty}^t \exp[-(t'' - t')/\tau_m] I_{P_{1,2}}(t') dt' \}^2 dt'' \quad (1)$$

where I_{P_3} and $I_{P_{1,2}}$ are the intensities of the probe and pump pulses, respectively. $\chi_{ijkl}^{(3)}(m)$ is a tensor element of the nonlinear optical susceptibility due to the process m with a decay time τ_m and a weighting factor C_m . These processes are the electronic ($m = e$) and the nuclear ($m = n$) optical Kerr effects (OKE) from the matrix or the solvent, the formation of a population grating ($m = p$), and the generation of a density grating due to heat releases ($m = d$).¹⁹ These four processes lead to four $\chi^{(3)}(m)$ tensors with different symmetry properties which can in principle be distinguished by using various combinations of polarization for the three pulses and by selecting a given polarization component of the signal.^{18,19} The second integral in eq 1 represents the convolution of the nonlinear response with the pump pulses, while the first integral is the convolution with the probe pulse.

The time profiles of the diffracted intensity were analyzed by iterative reconvolution using eq 1. The temporal width of the pump and probe pulses was determined by performing measurements with a solution of CV in MeOH. The ground-state recovery of CV in MeOH is known to take place in less than 3 ps, i.e., much faster than the response time of the experiment.²⁰ With our experimental setup and with a careful

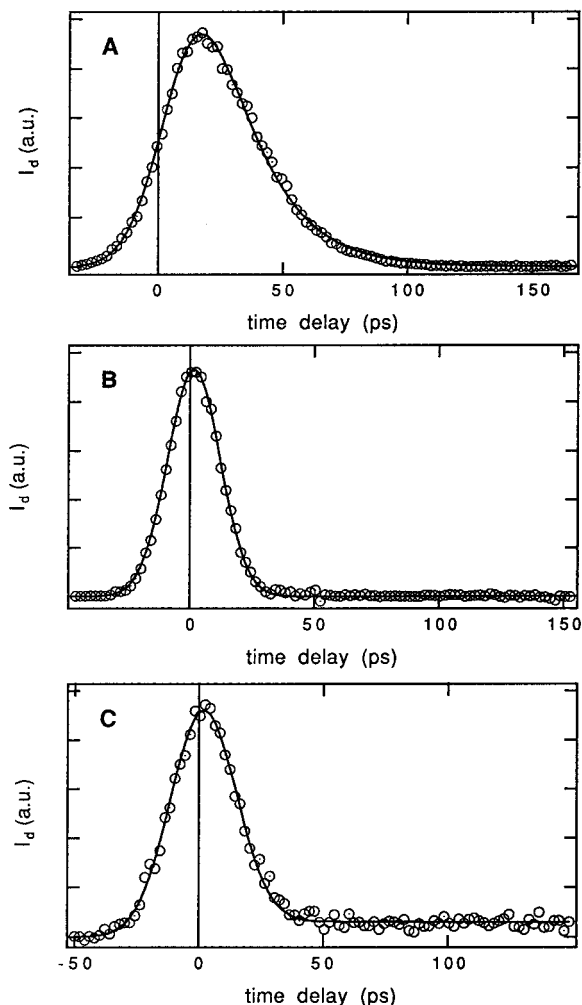


Figure 2. Time profiles of the diffracted intensity measured at 532 nm and best fits of eq 1 with (A) Pe^{+} in boric acid glass, (B) Pe^{+} in H_2SO_4 , and (C) Pe^{+} generated by photoinduced ET with DMA.

analysis of the time profile, the smallest resolvable decay time was of the order of 15 ps.

Results and Discussion

Pe^{+} in Boric Acid Glass. Figure 2a shows the time dependence of the diffracted intensity obtained by pumping and probing Pe^{+} in boric acid glass at 532 nm using the configuration described in Figure 1a. This time profile could be satisfactorily fitted using eq 1 assuming the contribution of a single process to the signal with a decay time of 35 ± 3 ps. This process corresponds to the ground-state recovery of Pe^{+} after excitation from D_0 to D_5 .²¹ To check for a possible contribution of the Kerr effect to this signal, the experiment was repeated on a region of the sample that had not been previously irradiated with UV light, i.e., that had no absorbance at 532 nm. With the pump-probe pulse intensity used previously, no signal could be detected. A signal could only be observed by increasing substantially the laser pulse intensity. Finally, the contribution of a density grating due to the heat released upon nonradiative transition to the ground state could only be observed at much larger time delays ($t > 3$ ns). Indeed, with a crossing angle of 2° , the acoustic period is of the order of 15 ns. Even at these time delays, the diffracted intensity due to the density grating was very small compared to that shown in Figure 2a. This can be understood by considering that the thermal expansion coefficient of boric acid glass must be similar to that of other glasses, i.e., about 100 times smaller

than that of organic solvents.²² For measuring the time profile shown in Figure 2a, the three pulses were polarized in the same direction, and therefore this profile reflects the dynamics of $\chi_{1111}^{(3)}(p)$. Other polarization combinations were used to probe $\chi_{1122}^{(3)}$ and $\chi_{1212}^{(3)}$ and resulted in a weaker signal but with the same temporal shape. Finally, to eliminate the possible contribution of gratings formed between one of the pump pulse and the probe pulse at time zero, the ground-state recovery of Pe^{+} was also probed at 545 nm. The decay of the time profile was the same, within the experimental error, as that measured at 532 nm.

Pe^{+} in Sulfuric Acid. The absorption spectrum in sulfuric acid depends on the concentration of Pe. At low concentration ($[\text{Pe}] = 10^{-5}$ M), the absorption spectrum was similar to that observed in boric acid glass, with the intense band located at 538 nm.²³ At higher concentration ($[\text{Pe}] = 10^{-3}$ M), a band with a maximum at 505 nm could also be observed. This band had previously been assigned to the dimer $(\text{Pe}^{+})_2$ which is in equilibrium with Pe^{+} .²⁴ The time profile of the diffracted intensity depicted in Figure 2b shows that the ground-state recovery of Pe^{+} in H_2SO_4 is faster than the response of the instrument and must therefore take place in less than 15 ps. For this measurement the concentration of Pe was 2×10^{-5} M. The experiment was repeated with a 10^{-2} M Pe solution using a 0.01 mm optical path length. At this concentration, the absorbance at 532 nm was mainly due to $(\text{Pe}^{+})_2$. In this case as well, the decay time of the diffracted intensity was shorter than 15 ps.

$\text{Pe}^{\bullet+}$, $\text{Pe}^{\bullet-}$, and $\text{AQ}^{\bullet-}$ in MeCN. These radical ions were generated by photoinduced intermolecular ET reaction. The pulse sequence is illustrated in Figure 1b. A UV pulse at 355 nm (P_4) excited either Pe or AQ dissolved in MeCN in the presence of either an electron donor (D) or an electron acceptor (A) with a concentration lying between 0.1 and 0.2 M. At this quencher concentration, the ET quenching takes place in less than a nanosecond, the reaction being diffusion controlled. Mataga and co-workers²⁵ have shown that for the Pe/TCNE pair, where TCNE is the electron acceptor, free Pe^{+} and $\text{TCNE}^{\bullet-}$ ions are formed within less than 5 ns with a yield of about 50%. Similarly, with the Pe/DMA pair, where DMA is the electron donor, free $\text{Pe}^{\bullet-}$ and $\text{DMA}^{\bullet+}$ ions are generated in the same time scale with a yield of about 70%. Finally, $\text{AQ}^{\bullet-}$ was generated by photoinduced ET between $^3\text{AQ}^*$ and DABCO with a resulting free ion yield close to unity.²⁶ These free ion populations decay in the microsecond time scale by homogeneous recombination.²⁷ As shown in Figure 1b, the transient grating experiment was performed on the free ion population 7 ns after the starting of the ET reaction by P_4 . At this time delay, the transient absorbance at 532 nm was of the order of 0.1 and remained constant within the time window of the transient grating experiment. The transient gratings were probed at both 532 and 545 nm. At those wavelengths, the absorption is due to either Pe^{+} or $\text{Pe}^{\bullet-}$ or $\text{AQ}^{\bullet-}$ but not to the corresponding quencher radical ion.¹⁶ Figure 2c shows the time profile measured at 545 nm with the Pe/DMA pair. After a decay that is too fast to be resolved, the diffracted intensity remained constant and larger than zero even at time delays larger than 1 ns (not shown). The nature of this very slow component will be discussed below. With Pe/TCNE, only the very fast decay was observed, indicating that the lifetime of Pe^{+} in MeCN is shorter than 15 ps.

For the AQ/DABCO pair, the time profile of the diffracted intensity was similar to that observed with the Pe/TCNE pair. However, a higher pulse intensity at 532 nm had to be used as the extinction coefficient of $\text{AQ}^{\bullet-}$ at this wavelength is

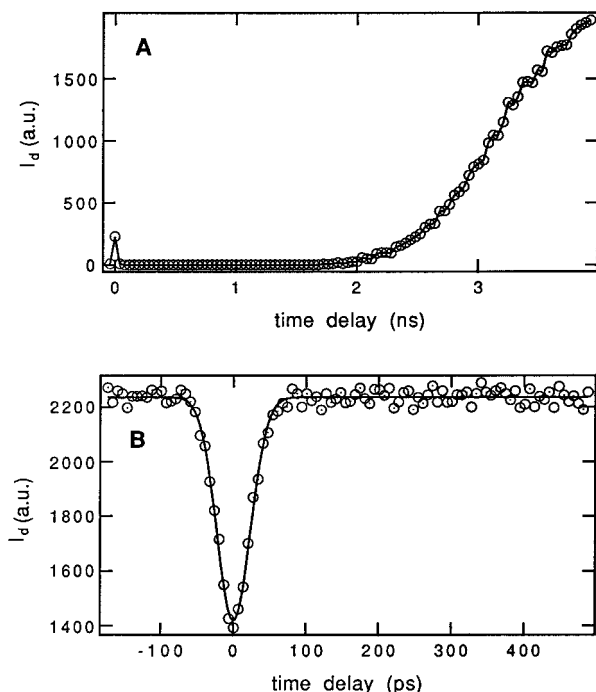


Figure 3. (A) Time profiles of the diffracted intensity measured at 532 nm with $\text{AQ}^{\bullet-}$ generated by photoinduced ET reaction with DABCO. (B) Dynamics of ground-state recovery of $\text{AQ}^{\bullet-}$ obtained by probing the density grating formed at different time delays after the bleaching pulse P_5 and best fit of a Gaussian function.

substantially smaller than that of Pe^{+} . For this reason, a diffracted signal could already be observed without the UV pulse, indicating the contribution from other processes than the population grating. This unwanted signal could not be totally eliminated even by using a combination of polarization to suppress the contribution of the nuclear OKE,^{18,19} indicating the occurrence of electronic OKE. In a polarization selective transient grating experiment, the contribution of electronic OKE cannot be distinguished from that of the population grating when the transition dipole involved in the pumping process is parallel to that involved in the probing process, as in the present case.¹⁹ Consequently, a different experiment was performed to measure the contribution of the population grating only, without those due to nonresonant nonlinear processes.

Dynamics of Ground-State Recovery by Monitoring $\chi_{ijkl}^{(3)}(d)$. Figure 3a shows the time profile of the diffracted intensity measured with the AQ/DABCO pair on a long time scale using parallel polarization. The slow rise of the diffracted intensity originates from $\chi_{1111}^{(3)}(d)$, i.e., from the density grating, which is itself caused by the thermal expansion following the nonradiative deactivation of $\text{AQ}^{\bullet-}$ to D_0 . The amplitude of this density grating and thus the diffracted intensity oscillate at a frequency $\omega = 4\pi \sin(\theta/2)v_s/\lambda_{\text{pu}}$,²⁸ where θ is the crossing angle of P_1 and P_2 at the wavelength λ_{pu} and v_s is the velocity of sound. In MeCN and with $\theta = 2^\circ$, the maximum of the first oscillation appears at a time delay of about 7 ns. The magnitude of this maximum is proportional to the square of the population of ions that have undergone photoexcitation and relaxation to the D_0 state and does not depend on any nonresonant processes. Therefore, the ground-state recovery dynamics of the ions was measured by monitoring $\chi_{1111}^{(3)}(d)$ using pulse sequence depicted in Figure 1c. The photoinduced ET reaction was triggered by the UV pulse, P_4 , and approximately 7 ns later, the absorbance at 532 nm due to free ion population was bleached by a single intense pulse at 532 nm (P_5 , 500 μJ , 2 mm beam radius). The dynamics of ground-state recovery was

monitored by measuring with P_3 the amplitude of the density grating, i.e., $\chi_{1111}^{(3)}(d)$, generated by the P_1 and P_2 pulses on the remaining ground-state ion population. The time delay between the $\text{P}_{1,2}$ pulses and the probe pulse P_3 was 7 ns. The bleaching pulse P_5 arrived on the sample at a variable time delay relative to the three transient grating pulses. This technique can be considered as flash photolysis with calorimetric detection.⁴² The advantage of monitoring the density grating instead of using a photoacoustic detector is that the heat generated by P_4 and P_5 does not contribute to the signal.^{30,31} Figure 3b shows the diffracted intensity measured with the AQ/DABCO pair as a function of the time delay between P_5 and the grating pulses, $\text{P}_{1,2}$. When the latter pulses arrive on the sample before P_5 , the absorbance at 532 nm is the highest and the amplitude of the density grating is the highest as well. When P_5 and $\text{P}_{1,2}$ are time coincident, the amplitude of the density grating is smaller, because the absorbance at 532 nm has been reduced by P_5 . Once the ground-state population of the ions and the absorbance at 532 nm have been restored, the amplitude of the density grating recovers its initial value. The continuous line in Figure 3b is the best fit of a Gaussian function. Time profiles with the same widths were obtained with CV in MeOH and with Pe/TCNE in MeCN. These measurements indicate that the lifetime of $\text{AQ}^{\bullet-}$ in MeCN is also shorter than the response time of the experiment. This result contrasts remarkably with the lifetime of 4 ns obtained indirectly by Fujita et al.¹¹ The origin of this discrepancy is not understood and might be due to the complexity of the system used by these authors.

Origin of the Incomplete Ground-State Recovery of $\text{Pe}^{\bullet-}$.

With the Pe/DMA system, the ground-state recovery of $\text{Pe}^{\bullet-}$ is not complete, indicating that a fraction of the anion population has undergone an irreversible photoreaction. By comparing the square root of the intensity of the fast and of the slow components of the time profile shown in Figure 2c, the quantum yield of this reaction is about 0.15, and therefore the time constant for this process must be shorter than 85 ps. As the overall concentration of Pe stays unchanged even after intense laser irradiation, the process responsible for the uncompleted recovery of the $\text{Pe}^{\bullet-}$ population must lead to the formation of neutral parent. Considering the time constant of this reaction and the concentrations of both $\text{DMA}^{\bullet+}$ and DMA, bimolecular processes such as $\text{Pe}^{\bullet-} + \text{DMA}^{\bullet+} \rightarrow \text{Pe} + \text{DMA}$ or $\text{Pe}^{\bullet-} + \text{DMA} \rightarrow \text{Pe} + \text{DMA}^{\bullet-}$ can be excluded. Consequently, the most probable process is electron photoejection from $\text{Pe}^{\bullet-}$, which is known to be a major deactivation pathway of photoexcited radical anions in the gas phase and in nonpolar solvents.⁶ For example, a photoejection yield of 0.46 has been reported for $\text{Pe}^{\bullet-}$ in tetramethylsilane.³² In the gas phase, photoejection takes place when the excitation energy is larger than the electron affinity of the neutral parent molecule. In the case of $\text{Pe}^{\bullet-}$ and $\text{AQ}^{\bullet-}$, this should take place upon excitation at wavelengths below 1400 and 780 nm, respectively.^{32,33} In solution and particularly in polar solvents, the ions are stabilized, and the threshold energy for photoejection, E_{th} , can be expressed as^{11,32}

$$E_{\text{th}} = E_{\text{red}} + V_0 + C \quad (2)$$

where E_{red} is the reduction potential of the parent neutral in MeCN ($E_{\text{red}}(\text{Pe}) = -1.66$ V vs SCE,³⁴ $E_{\text{red}}(\text{AQ}) = -0.894$ V vs SCE³⁵), V_0 is the lower edge of the conduction band of an electron in the solvent relative to vacuum ($V_0 = -0.14$ eV in MeCN³⁶), and C is the oxidation potential of a reference calomel electrode ($C = 4.56$ V). From this equation, E_{th} is equal to 2.7 eV for $\text{Pe}^{\bullet-}$ and to 3.5 eV for $\text{AQ}^{\bullet-}$. Comparison between these values and the energy of a photon at 532 nm ($E_{\text{hv}} = 2.33$ eV)

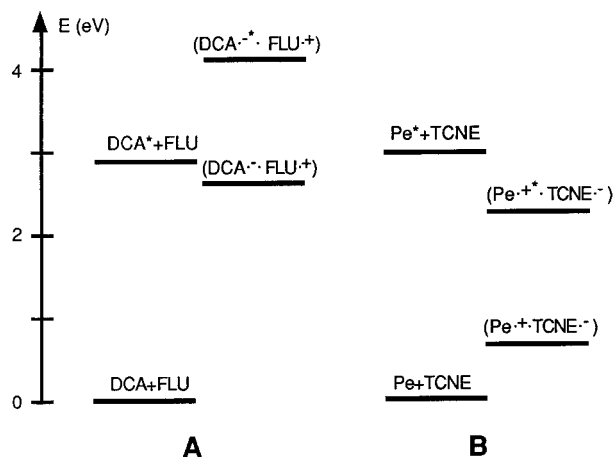


Figure 4. Energy levels involved in the photoinduced ET reaction in MeCN between (A) DCA and FLU and (B) perylene and TCNE.

shows that photoejection with a single photon is not possible with $AQ^{•-}$. On the other hand, considering the uncertainties of the values used in the calculation, the threshold for $Pe^{•-}$ is close to the energy of a 532 nm photon. For $Pe^{•-}$ in nonpolar solvents, the time constant for photoejection has been estimated to be smaller than 100 fs.³² Therefore, a time constant shorter than 85 ps is reasonable, even for an electron ejection with a photon close to the threshold energy. However, the occurrence of biphotonic ejection cannot be excluded.

ET Dynamics with Excited Ions. The free ion yield in an intermolecular ET reaction in solution depends on the competition between back ET within the ion pair and diffusion of the ions. In MeCN, diffusion of the ions out of the reaction volume, where geminate recombination is still possible, occurs within a couple of nanoseconds, whereas the rate constant of back ET is very sensitive to the energy gap between the ion pair state and the neutral ground state.^{25,37–39} Consequently, if one of the ions within the geminate ion pair is in an electronic excited state, the energy gap for back ET is substantially larger than the energy gap with both ions in the ground state. Of course, this additional free energy can only influence the free ion yield if the excited-state lifetime of the ion is not too small compared with the time scale of ion diffusion. For example, if the excited-state lifetime of $DCA^{•+}$ is around 5 ns, as determined by Fujita et al.,¹¹ excitation of $DCA^{•+}$ within the geminate ion pair ($DCA^{•+} \cdot D^{•+}$) formed after ET quenching should influence the free ion yield. Such an experiment was performed with two electron donors, FLU and ANI. The free energy for back ET from the ion pair in the ground state amounts to about -2.63 and -2.74 eV for FLU and ANI, respectively (see Figure 4a). Upon excitation at 355 nm with a 20 ns laser pulse of a solution of a DCA containing 0.2 M donor in MeCN, the free ion yield was around 20% and 14% with FLU and ANI, respectively. The absorbance at 532 nm after 355 nm excitation was of the order of 0.1. The same experiment was repeated with an additional, time coincident, 20 ns laser pulse at 532 nm to excite $DCA^{•+}$. Back ET within ($DCA^{•+} \cdot D^{•+}$) to the neutral ground state is more negative by 1.56 eV²¹ than back ET within ($DCA^{•+} \cdot D^{•+}$) and should consequently be much slower. On the other hand, back ET to $DCA^+ + D$ is not possible from ($DCA^{•+} \cdot D^{•+}$) but is energetically feasible from ($DCA^{•+} \cdot D^{•+}$), the corresponding free energy being equal to -1.30 and -1.41 eV for FLU and ANI, respectively (see Figure 4a). Consequently, this very different situation for recombination within ($DCA^{•+} \cdot D^{•+}$) should have a strong repercussion on the free ion yield, as long as the lifetime of $DCA^{•+}$ is long enough. The intensity ratio of the 532 nm/355 nm laser pulse intensity was varied from 0.2 to 2. With this additional excitation, the

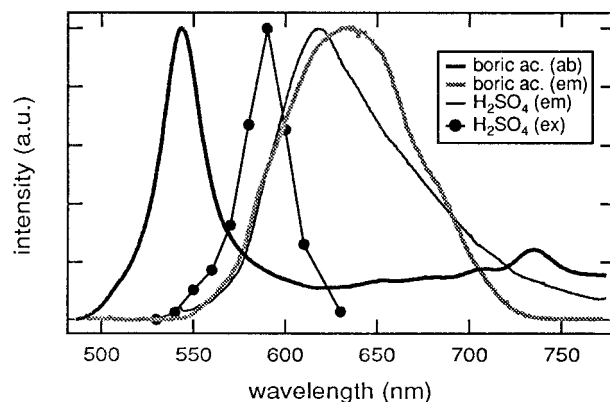


Figure 5. Absorption spectrum of Pe-doped boric acid glass after UV irradiation (thick black line), emission spectrum measured with the same sample upon excitation at 532 nm (thick gray line), emission spectrum measured with a solution of Pe in H_2SO_4 excited at 532 nm (thin black line), and corresponding excitation spectrum (black dots).

free ion yields were identical with those obtained without the 532 nm pulse. No effect was observed with the Pe/TCNE pair either (see Figure 4b). The latter result was expected as the lifetime of $Pe^{•+}$ has been measured to be shorter than 15 ps. The result with DCA strongly suggests that the lifetime of $DCA^{•+}$ is much smaller than 5 ns.

Emission from Radical Ions. Upon laser irradiation at 532 nm, the $Pe^{•+}$ -doped boric acid glasses exhibited a weak red luminescence which is shown in Figure 5. Its intensity was too small to perform an excitation spectrum. However, $Pe^{•+}$ in H_2SO_4 exhibited a similar emission which was intense enough to measure an excitation spectrum which is also shown in Figure 5. This spectrum coincides very well with the absorption spectrum of protonated perylene, PeH^+ , measured in HF solution.²³ Recently, similar absorption and emission spectra were observed with Pe in zeolites and were indeed ascribed to PeH^+ .⁴⁰ As the absorption band of PeH^+ around 600 nm is completely hidden by those of $Pe^{•+}$, the concentration of the protonated Pe in both boric acid glass and in H_2SO_4 must be very small compared to that of the radical cation. Moreover, the absorbance of PeH^+ at 532 nm is close to zero, and therefore this species does not play any role in the ground-state recovery measurements.

The fluorescence of $Pe^{•+}$ has been reported in BF_3 -trifluoroacetic acid solution, on surfaces⁹ and in rare gas matrixes at low temperature.⁴¹ The solution and surface fluorescence spectra consist of two bands, one located around 800–820 nm and a second one at 910 nm. In H_2SO_4 and in boric acid glass, the presence of the emission band of $PeH^{•+}$ and of other bands observed with undoped boric acid glass did not allow a unequivocal detection of fluorescence from $Pe^{•+}$. The intensity of $Pe^{•+} D_1 \leftarrow D_0$ absorption band is very weak and corresponds to an oscillator strength of the order of 5×10^{-3} .²¹ From this value, the natural radiative lifetime of $Pe^{•+}$ can be calculated to be of the order of 1 μs . Such a very long natural radiative lifetime, together with a nonradiative decay time in solution of a few picoseconds, indicates a fluorescence quantum yield of the order of 10^{-6} . Similar fluorescence quantum yields are predicted for $Pe^{•+}$ and $AQ^{•+}$, which should fluoresce above 1100 nm. The detection of such weak emissions is certainly possible, but only with samples of well-known composition and that do not contain other fluorescing species. The systems studied here are therefore not well suited for such measurements.

Concluding Remarks

The very fast ground-state recovery of the ions measured here must be due to a very efficient internal conversion favored by

a small D_1 – D_0 energy gap. This property seems to be a general characteristic of almost all organic radical ions, and therefore short excited-state lifetimes have to be expected for most of them. Coincidentally, the oscillator strength of the $D_1 \leftarrow D_0$ transition of many radical ions is small, indicating a long natural radiative lifetime. Consequently, the detection of the fluorescence of most radical ions requires laser excitation and also near-IR detection. This certainly explains why so few genuine emission from radical ions in the condensed phase at room temperature have been reported so far.

The different lifetimes of $\text{Pe}^{\bullet+}$ measured in boric acid glass and liquid solutions must be due to the fact that the coupling between the vibrational modes of the ions and the phonons of the medium is less efficient in the glass than in the liquids. In rare gas matrixes at low temperature, this coupling is so weak that vibrationally unrelaxed fluorescence has been observed for substituted benzene cations.⁶ The same effect might explain the observation of the fluorescence of $\text{Pe}^{\bullet+}$ on surfaces.⁹

Considering the small $D_1 \leftarrow D_0$ energy gap of most aromatic radical ions involved in ET quenching experiments, the formation of excited radical ions in exergonic processes is not only energetically feasible (see for example Figure 4b) but also should be favored by a superior vibronic coupling with respect to the formation of the ions in the ground state. However, the very short lifetime of excited radical ions makes the detection of such intermediates extremely difficult.

Acknowledgment. This work was supported by the Fonds national suisse de la recherche scientifique through Project No. 20-49235.96 and by the program d'encouragement à la relève universitaire de la Confédération. Financial support from the Fonds de la recherche and the Conseil de l'Université de Fribourg is also acknowledged.

References and Notes

- Haselbach, E.; Bally, T. *Pure Appl. Chem.* **1984**, *56*, 1203.
- Mataga, N.; Kanda, Y.; Asahi, T.; Miyasaka, H.; Okada, T.; Kakitani, T. *Chem. Phys.* **1988**, *127*, 239.
- Kikuchi, K.; Katagiri, T.; Niwa, T.; Takachi, Y.; Suzuki, T.; Ikeda, U.; Miyashi, T. *Chem. Phys. Lett.* **1992**, *193*, 155.
- Miller, T. A. *Annu. Rev. Phys. Chem.* **1982**, *33*, 257.
- Klapstein, D.; Maier, J. P.; Misev, L. In *Molecular Ions: Spectroscopy, Structure and Chemistry*; Miller, T. A., Bondibey, V. E., Eds.; North-Holland: Amsterdam, 1983; p 175.
- Bondibey, V. E.; Miller, T. A. In *Molecular Ions: Spectroscopy, Structure and Chemistry*; Miller, T. A., Bondibey, V. E., Eds.; North-Holland: Amsterdam, 1983; p 125.
- Eriksen, J.; Lund, H.; Nyvad, A. *Acta Chem. Scand.* **1983**, *B37*, 459.
- Eriksen, J.; Jorgensen, K. A.; Lindenberg, J.; Lund, H. *J. Am. Chem. Soc.* **1984**, *106*, 5084.
- Pankasem, S.; Iu, K. K.; Thomas, J. K. *J. Photochem. Photobiol. A* **1991**, *62*, 53.
- Breslin, D. T.; Fox, M. A. *J. Phys. Chem.* **1994**, *98*, 408.
- Fujita, M.; Ishida, A.; Majima, T.; Takamuka, S. *J. Phys. Chem.* **1996**, *100*, 5382.
- Vauthey, E. *Chem. Phys. Lett.* **1993**, *216*, 530.
- Högemann, C.; Pauchard, M.; Vauthey, E. *Rev. Sci. Instrum.* **1996**, *67*, 3449.
- von Raumer, M.; Suppan, P.; Jacques, P. *J. Photochem. Photobiol. A* **1997**, *105*, 21.
- Andreev, O. M.; Smirnov, V. A.; Alfimov, M. V. *J. Photochem.* **1977**, *7*, 149.
- Shida, T. *Electronic Absorption Spectra of Radical Ions*; Elsevier: Amsterdam, 1988; Vol. Physical Sciences Data 34.
- Shen, Y. R. *The Principles of Nonlinear Spectroscopy*; J. Wiley: New York, 1984.
- Etchepare, J.; Grillon, G.; Chambaret, J. P.; Hamoniaux, G.; Orzag, A. *Opt. Commun.* **1987**, *63*, 329.
- Deeg, F. W.; Fayer, M. D. *J. Chem. Phys.* **1989**, *91*, 2269.
- Sundström, V.; Gillbro, T. In *Picosecond Chemistry and Biology*; Doust, T. A. M., West, M. A., Eds.; Science Review: Northwood, 1983; p 148.
- Negri, F.; Zgierski, M. Z. *J. Chem. Phys.* **1994**, *100*, 1387.
- Handbook of Chemistry and Physics*, 66th ed.; CRC Press: Boca Raton, FL, 1985.
- Aalbersberg, W. I.; Hoijsink, G. J.; Mackor, E. L.; Weiland, W. P. *J. Chem. Soc.* **1959**, 3049.
- Kimura, K.; Yamazaki, T.; Katsumata, S. *J. Phys. Chem.* **1971**, *75*, 1768.
- Mataga, N.; Asahi, T.; Kanda, Y.; Okada, T.; Kakitani, T. *Chem. Phys.* **1988**, *127*, 249.
- Haselbach, E.; Vauthey, E.; Suppan, P. *Tetrahedron* **1988**, *44*, 7335.
- Haselbach, E.; Jacques, P.; Pilloud, D.; Suppan, P.; Vauthey, E. *J. Phys. Chem.* **1991**, *95*, 7115.
- Nelson, K. A.; Fayer, M. D. *J. Chem. Phys.* **1982**, *79*, 5202.
- Terazima, M. *J. Phys. Chem.* **1997**, *101*, 3227.
- Rothberg, L. J.; Bernstein, M.; Peters, K. S. *J. Chem. Phys.* **1983**, *79*, 2569.
- Siegman, A. E. In *Applications of Picosecond Spectroscopy to Chemistry*; Eisenthal, K. B., Ed.; D. Reidel: Dordrecht, 1983; p 325.
- Sowada, U.; Holroyd, R. A. *J. Phys. Chem.* **1981**, *85*, 541.
- Kebarle, P.; Chowdhury, S. *Chem. Rev. (Washington, D.C.)* **1987**, *87*, 513.
- Parker, V. D. *J. Am. Chem. Soc.* **1976**, *98*, 98.
- Peover, M. E. *J. Chem. Soc.* **1962**, 4541.
- Peover, M. E. *Electrochim. Acta* **1968**, *13*, 1083.
- Marcus, R. A.; Sutin, N. *Biochim. Biophys. Acta* **1985**, *811*, 265.
- Gould, I. R.; Ege, D.; Mattes, S. L.; Farid, S. *J. Am. Chem. Soc.* **1987**, *109*, 3794.
- Vauthey, E.; Suppan, P.; Haselbach, E. *Helv. Chim. Acta* **1988**, *71*, 93.
- Iu, K. K.; Liu, X.; Thomas, J. K. *Chem. Phys. Lett.* **1991**, *186*, 198.
- Joblin, C.; Salama, F.; Allamandola, L. *J. Chem. Phys.* **1995**, *102*, 9743.
- This technique is very similar to a method described by Terazima²⁹ in a paper which was published while we were writing this one.